Embryonic and foetal expression patterns of the ciliopathy gene *CEP164*

Devlin LA[1], Ramsbottom SA[1], Overman LM[2], Lisgo SN[2], Clowry G[3], Molinari E[1], Miles CG[1], Sayer JA[1,,4,5*].

Author information

Affiliations

1. Institute of Genetic Medicine, Newcastle University, Central Parkway, Newcastle upon Tyne, NE1 3BZ, United Kingdom.
2. MRC-Wellcome Trust Human Developmental Biology Resource, Institute of Genetic Medicine, International Centre for Life, Newcastle upon Tyne, NE1 3BZ
3. Institute of Neuroscience, The Medical School, Newcastle University, Framlington Place, Newcastle upon Tyne, NE3 4HH, United Kingdom.
4. The Newcastle upon Tyne Hospitals NHS Foundation Trust, Freeman Road, Newcastle upon Tyne, NE7 7DN, United Kingdom.
5. National Institute for Health Research Newcastle Biomedical Research Centre, Newcastle upon Tyne, NE4 5PL, United Kingdom.

Corresponding author

*Correspondence to John A. Sayer

Institute of Genetic Medicine, Newcastle University, Central Parkway, Newcastle upon Tyne, NE1 3BZ, United Kingdom

Tel +44 191 2418608

John.sayer@ncl.ac.uk

Abstract

Nephronophthisis-related ciliopathies (NPHP-RC) are a group of inherited genetic disorders that share a defect in the formation, maintenance or functioning of the primary cilium complex, causing progressive kidney failure and other clinical manifestations. Mutations in centrosomal protein 164 kDa (*CEP164*), also known as *NPHP15*, have been identified as a cause of NPHP-RC. Here we have utilised the MRC-Wellcome Trust Human Developmental Biology Resource (HDBR) to perform immunohistochemistry studies on human embryonic and foetal tissues to determine the expression patterns of *CEP164* during development. Notably expression is widespread, yet defined, in multiple organs including the kidney, retina and cerebellum. Murine studies demonstrated an almost identical *Cep164* expression pattern. Taken together, this data supports conserved roles for *CEP164* throughout the development of numerous organs, which we suggest accounts for the multi-system disease phenotype of *CEP164* mediated NPHP-RC.

Keywords: cilia, nephronophthisis, gene expression, CEP164, Joubert syndrome, development

Introduction

Nephronophthisis-related ciliopathies (NPHP-RC) are a collection of inherited genetic disorders, grouped together by a core defect in the formation, maintenance or functioning of the primary cilium complex [1, 2]. NPHP-RC patients typically present with nephronophthisis, a fibrotic cortico-medullary cystic kidney phenotype, which frequently leads to end stage-renal disease (ESRD) [3, 4]. In some NPHP-RC cases, including Senior-Loken syndrome (SLSN), Alstrom syndrome (AS), Bardet Biedl syndrome (BBS) and Joubert syndrome (JBTS), patients have retinal dysplasia and degeneration phenotypes, such as Leber congenital amaurosis, which can deteriorate to blindness [5-7]. Neurological abnormalities are often present; JBTS patients have midbrain cerebellar vermis hypoplasia, characterised by the "molar tooth" sign on MRI analysis [5, 8]. This can cause numerous problems including ataxia, hypotonia and breathing abnormalities. Intellectual disability and developmental delay can also be present, which is demonstrated throughout the spectrum of NPHP-RC. Additionally, BBS patients are often diagnosed with hypogonadism and/or obesity [9]. Severe NPHP-RC phenotypes, including Jeune syndrome and Meckel Gruber syndrome, can also present with skeletal dysplasia, and lethal occipital encephalocele. Consistent with ciliopathy syndromes, polydactyly, liver fibrosis, facial dysmorphism, cardiac abnormalities, hearing loss and type 2 diabetes can present as secondary symptoms [9-11]. Although some disease management therapies are available, notably, there is no cure for NPHP-RC.

There are at least 25 NPHP-RC causative genes currently identified [12], accounting for a molecular genetic diagnosis in around 60% of NPHP-RC patients. Mutations in *CEP164*, also known as *NPHP15*, have been identified as a cause of NPHP-RC [1, 9]. These patients

have a largely heterogenous clinical presentation. The majority suffer with NPHP and a retinal phenotype, which is some patients cause blindness prior to two years of age. One patient was diagnosed with JBTS, and two others have BBS-like manifestations with an absence of renal problems [1, 9]. It has been proposed that homozygous truncating mutations of *CEP164*, cause a severe JBTS phenotype, whereas hypomorphic mutations may cause a less severe phenotype [1]. Patients with identical *CEP164* mutations can display different clinical manifestations, which makes it difficult to understand the pathology and progression of the disease.

CEP164 was first identified and cloned from an adult foetal brain cDNA library [13] and is located on chromosome 11, q23.3. Its largest, most commonly cited isoform is 5,629 bp, encoding the 1,460 amino acid protein (CEP164) (NM_014956) [1, 14]. There is an alternative isoform of CEP164 (NM_001271933), with a 1,455 amino acid product [1, 13, 14]. CEP164 is a centrosomal protein that localises to each of the nine distal appendages of the primary cilia mature centriole, in a microtubule-independent manner [1, 2, 15-22] . This has been demonstrated by super-resolution microscopy techniques in multiple human and murine cell lines. Cell-cycle dependent recruitment of CEP164 to the basal body distal appendages is hierarchical, within a network of other distal appendage proteins. These include CEP83 (mutations in *CEP83* cause NPHP18), CEP89, SCLT1 (variants in SCLT1 may be associated with OFD IX), and FBF1. CEP164 is recruited last, defining the proximal end of the transition zone [2, 15, 18, 22-26].

Proteomics analysis has identified that CEP164 has an N-terminal tryptophan-tryptophan (WW) domain, an area of lysine-rich repeats (LR), and multiple serine/glutamine (SQ/TQ)

97 potential phosphorylation sites [2, 14]. There are at least 3 predicted coiled-coil domains [1,
98 2, 14, 15] and the C-terminal domain is currently undefined. (**S1 Figure A**). Multiple fusion
99 protein studies have demonstrated that the CEP164 C-terminal domain is required for
100 localisation of CEP164 to the distal appendages [1, 15]. Additionally, CEP164 has been
101 localised to the nucleus [1, 14, 17, 27].

102

103 Numerous *CEP164* knockdown studies (siRNA/CRISPR) have demonstrated that *CEP164*
104 loss causes aberration of ciliogenesis, with disruption of primary cilia production prior to
105 transition zone formation; notably centriolar structure is not disrupted [15, 23, 25, 28, 29].
106 Upon initiation of ciliogenesis Rabin 11 imports the GTPase Rabin 8 to the basal body.
107 CEP164 interacts with Rabin 8, facilitated by Chibby 1, to recruit Rab8 positive vesicles to
108 the centrosome [15, 17, 19, 24, 30]. Vesicle docking is required for subsequent basal body
109 anchoring to the plasma membrane and primary cilia development. Additionally, CEP164
110 forms a complex with tau tubulin kinase 2 (TTBK2) via its N-terminal WW domain. CEP164
111 recruits TTBK2 to the primary cilia basal body, which allows removal of the centriolar
112 capping protein, CP110, potentially via phosphorylation, initiation of intraflagellar transport
113 recruitment and subsequent axonemal extension [1, 15, 29, 31, 32]. The CEP164/Rabin 8 and
114 CEP164/TTBK2 pathways work independently of each other [29]. There are other predicted
115 interactors of CEP164 including dishevelled, NPHP3, NPHP4 and ARL13B, indicating that
116 CEP164 is likely to have other ciliary roles [1, 15, 24, 32].

117

118 Several studies have indicated a potential role for CEP164 in ATM/ATR-mediated DNA
119 damage response (DDR) and UV-induced nucleotide excision repair pathways, however
120 results are conflicting [14, 17, 33]. Likewise, data supporting a role for CEP164 in cell-cycle

121 regulation is inconsistent [1, 2, 14, 15, 25]; both of these CEP164 roles need to be further
122 validated.

123

124 *CEP164* has numerous orthologs, including *M.muscularis, D.melanogaster, C.reinhardtii*
125 *and D.rerio* (**S1 Figure B,C,D**). The murine ortholog of *CEP164* is a 30-exon gene, located
126 on chromosome 9, qA5.2, which shares 77% identity to the full-length human *CEP164.* It
127 encodes a 1333 amino acid protein, which shares 58% identity to the human CEP164 1,460
128 amino acid protein [34, 35]. Like human *CEP164,* murine *Cep164* may have multiple
129 isoforms.

130

131 Given *CEP164* mutations cause NPHP-RC, we sought to determine the expression of
132 *CEP164* throughout human and murine development, particularly focusing on the cerebellar-
133 retinal-renal phenotype. Collaboration with the Medical Research Council (MRC) Human
134 Developmental Biology Resource (HDBR) allowed the procurement of human embryonic
135 and foetal samples, which was compared to expression data from the murine 129/OlaHsd-
136 *Cep164*$^{tm1a(EUCOMM)Wtsi/+}$ gene trap model.

137

138

139

140

141

142

Materials and Methods

Study approval. The study was conducted with full ethical approval and consent. Ethical approval was obtained from the National Research Ethics Service Committee North East – Newcastle & North Tyneside 1 (08/H0906/21+5). Human embryonic and foetal tissue samples were collected with appropriate consent and ethical approval, via the Medical Research Council (MRC) Wellcome trust-funded Human Developmental Biology Resource (HDBR). Animal experiments were performed under Home Office Licences (United Kingdom) in accordance with the guidelines and regulations for the care and use of laboratory animals outlined by the Animals (Scientific Procedures) Act 1986. Protocols conducted were approved by the Animal Ethics Committee of Newcastle University and the Home Office, United Kingdom.

Mouse Genetics. *C57BL/6NTac-Cep164*$^{tm1a(EUCOMM)Wtsi/+}$ mice, which were generated for the International Phenotyping Consortium Initiative, were obtained from MRC Harwell [36]. These were backcrossed onto a *129/Ola-Hsd* background, forming mice heterozygous for the gene trap, *129/OlaHsd-Cep164*$^{tm1a(EUCOMM)Wtsi/+}$. *129/OlaHsd-Cep164*$^{tm1a(EUCOMM)Wtsi/+}$ heterozygous (HET) mice were mated with wild type (WT) *129/OlaHsd-Cep164*$^{+/+}$ mice, gaining pups HET:WT 1:1. In the *Cep164*^{tm1a} allele, upon pre-mRNA processing, exon 3 of *Cep164* splices into the *LacZ/Neomycin* cassette, within intron 3, which introduces a frame-shift and subsequent nonsense mutations (**S2 Figure**). This generates a *Cep164* null allele by hypothesised nonsense mediated decay. The *LacZ* cassette contains an internal ribosomal entry site (IRES), allowing translation of a beta-galactosidase fusion gene upon activation of the native *Cep164* promoter, thus acting as a *Cep164* reporter gene. Upon additional of X-Gal substrate, beta galactosidase hydrolyses X-Gal forming 5-bromo-4-chloro-3-hydroxyindole-1,

which oxidises to a blue precipitate, 5,5'-dibromo-4,4'-dichloro-indigo-2. HET *129/OlaHsd-Cep164*$^{tm1a(EUCOMM)Wtsi/+}$ mice were used for X-Gal *Cep164* expression studies, as they are phenotypically normal, WT mice were used as littermate controls.

***Cep164* genotyping.** Ear or tail biopsies (embryos) were lysed for 1 h, at 95°C, in 50 µl alkaline lysis buffer (25 mM NaOH, 0.2 mM EDTA, pH ≈ 12) and then neutralised in 50 µl neutralising buffer (40 mM trizma hydrochloride, pH 5-5.5). A PCR reaction using GoTaq G2 DNA Polymerase (Promega) for *Cep164*$^{tm1a(EUCOMM)Wtsi/+}$, was completed using the following primers flanking the second loxp site; F1 5' CTC CCA CAG TGA CAA ATG CC 3', R1 5' GGT AGT TGT TAC TTC TGT CAG 3' (Eurofins Genomics). Expected amplicon sizes are as follows; WT (141 bp), homozygous (Hom) (163 bp), HET (141 bp and 163 bp). PCR products were run on a 1.5% agarose gel, with GelRed Nucleic Acid GelStain (1:10,000) (Biotium) at 150V for 45 min. To confirm correct genotyping, representative samples were Sanger-sequenced (GATC-BIOTECH).

Murine Tissue Collection, Fixation, Sectioning and Staining. Murine tissue (kidney, brain, eye, heart, lung, liver, testes) was collected at P0.5/P1.5, P15.5 and P29.5/P30.5, using a standard dissection procedure. Tissues were fixed in 0.2% glutaraldehyde fix (0.2% glutaraldehyde, 2mM $MgCl_2$, 5mM EGTA in PBS) for 90 min at 4°C, washed in PBS and then stored in 15% sucrose/PBS overnight at 4°C.Tissues were transferred to 30% sucrose/PBS and incubated at 4°C overnight or until samples sunk. Tissues were frozen in OCT compound, and stored at -80°C.

Sections of tissues were cut (10-12µm) using a cryostat and mounted on charged glass slides. These were incubated in 0.2% glutaraldehyde fix (0.2% glutaraldehyde, 2mM $MgCl_2$, 5mM EGTA in PBS) for 5 min, washed in PBS for 10 min, and then washed in X-Gal wash (2 mM $MgCl_2$, 0.01% Sodium Deoxycholate, 0.02% NP-40 in PBS) for 10 min. Slides were incubated with X-Gal stain (1mg/ml of X-Gal DMSO in 2 mM $MgCl_2$, 0.01% Sodium Deoxycholate, 0.02% NP-40, 5mM Potassium Ferricyanide, 5mM Potassium Ferrocyanide in PBS) at 37°C in the dark, until the blue precipitate stain intensity did not further increase or WT littermate controls showed endogenous beta galactosidase staining. Slides were washed in PBS and then dehydrated to 100% ethanol before clearing in Histoclear II (National Diagnostics) and mounting in DPX mounting medium (Sigma-Aldrich), slides were imaged using the SCN400 Side Scanner (Leica).

Murine Embryo Collection, Wholemount Fixation and Staining. Murine embryos were collected at E9.5, E10.5 and E12.5 using a standard dissection procedure. Embryos were fixed in 0.2% glutaraldehyde solution (0.2% glutaraldehyde, 2mM $MgCl_2$, 5mM EGTA in PBS) for 1 hour on ice and washed with X-Gal wash (2 mM $MgCl_2$, 0.01% Sodium Deoxycholate, 0.02% NP-40 in PBS) prior to overnight storage at 4°C. Embryos were incubated in X-Gal stain, consisting of 25mg/ml of X-Gal/DMSO solution in a 1 in 25 dilution of X-Gal staining buffer (2 mM $MgCl_2$, 0.01% Sodium Deoxycholate, 0.02% NP-40, 5mM Potassium Ferricyanide, 5mM Potassium Ferrocyanide in PBS) at 37°C in the dark; incubation was completed once the blue precipitate stain intensity did not further increase or WT littermate controls started to show endogenous beta galactosidase staining. Embryos were washed in 1x phosphate buffered saline solution (PBS) (Gibco, pH7.45) and dehydrated in 70% ethanol, prior to imaging using a Leica Man Stereomicroscope and Axiovision software.

Human Tissue collection, fixation and processing. Human embryonic and foetal tissues were obtained from the MRC Wellcome Trust-funded Human Developmental Biology Resource. CS23 whole embryos were fixed in 4% paraformaldehyde (PFA), for 72 hours, with incision in the skull down the sagittal plane and a slit in the abdomen at the umbilicus. Tissues were transferred to methacarn until further processed. This same protocol was used for processing of foetal eye, brain and kidney; the embryonic and foetal kidney were cut sagittally, to allow the fix to penetrate. Human embryonic and foetal tissues were washed in increasing concentrations of ethanol, and then incubated in 3 changes of xylene before embedding in paraffin wax. Sections, on positively charged glassed slides, were de-waxed in two washes of xylene, and then rinsed in two changes of absolute ethanol. Slides were incubated in methanol peroxide solution (0.5% H_2O_2) for 10 min to block endogenous peroxidase. Slides were rinsed in tap water and then antigen retrieval was completed using citrate buffer. After rinsing in Tris-buffered saline (TBS), slides were incubated with 10% goat serum (Vector) for 10 min at room temperature and then incubated with the primary antibody in goat serum with TBS overnight at 4 °C (**S1 Table**). After washing with TBS, slides were incubated with the goat anti rabbit BA-1000 biotinylated secondary antibody (Vector Laboratories) diluted in goat serum with TBS (1/500), for 30 min at room temperature. The secondary was washed with TBS and then slides were incubated with VECTASTAIN Elite ABC kit PK6100 tertiary complex (Vector Laboratories), for 30 min at room temperature. After TBS washes, the stain was developed for 10 min at room temperature using ImmPACT DAB peroxidase substrate (SK-6100) solution (Vector Laboratories). The slides were washed thoroughly in water, and counterstained with haematoxylin, dehydrated, cleared and mounted.

An indirect, two-step, method was utilised for the foetal kidney sections. Samples were incubated with a HRP goat anti-rabbit IgG peroxidase secondary (Vector) (1/500). After TBS washes, the stain was developed using DAB peroxidase substrate solution, as described previously. No primary controls sections were utilised as negative controls, anti-PAX6 was utilised as a positive control for the brain and cerebellum (**S1 Table**).

Image analysis. Images of human and murine tissues were analysed using the SCN400 Slide scanner software (Leica). Figures 1-4, and S3-S5 Figures were generated using Adobe Photoshop CS3 Extended.

Data Availability. The authors declare that all data supporting the results are presented with the article, supporting data can be gained from the corresponding author upon reasonable request.

Results

CEP164 expression during human and murine renal development

In the human embryonic and foetal kidney, immunohistochemical staining demonstrates that CEP164 is present in the metanephric epithelial-derived renal vesicles, comma-shaped bodies and subsequent s-shaped bodies, during all time points analysed (8PCW-18PCW) **(Figure. 1 A.I.II.III.VII B.I.II C.I.II).** This expression pattern is maintained throughout nephrogenesis, with CEP164 present in the primitive nephron tubule (8PCW), but also in more defined proximal and distal nephron segments, as well as cells of the loop of Henle, as seen from 14 PCW (**Figure 1A.I.IV.VII, B.I.IV.VII, C.I.IV.VII**). Specifically, CEP164 expression is

263 defined to the apical membrane of the epithelial cells lining the developing nephron lumen,
264 during all the developmental time points analysed (8PCW- 18PCW). Notably, CEP164
265 expression is stronger in the premature nephron renal vesicles, comma-shaped bodies, s-
266 shaped bodies and immature renal tubules, which is then reduced in the more developed
267 cortical and medullary tubular segments (8PCW-18PCW). CEP164 does not seem to be
268 expressed, or is expressed very weakly, in the metanephric cap mesenchyme (**Figure 1A.III,**
269 **B.III**).

270

271 **Figure 1. Expression of CEP164 throughout human and murine renal development**
272 (A-C) Human renal development, (A) 8 PCW, (B) 14 PCW and (C) 18 PCW respectively.
273 (D, E) Murine postnatal renal development, (D) P1.5 and (E) P30.5. In human kidney,
274 CEP164 is expression is seen in the apical membrane of the metanephric renal vesicles (A.II,
275 B.II), s-shaped bodies (B.II, C.I, C.II) and developing renal tubules (A.IV, B.IV). From 14
276 PCW CEP164 expression is seen at the apical membrane of all developing tubular segments
277 including the distal and proximal tubules, (B.IV, C.IV) and loop of Henle segments (B.VII,
278 C.VII). CEP164 expression is seen in the cells of the uteric bud (A.III, B.III, CII) at both the
279 apical and basal membrane (A.VII, B.VII, C.VII). CEP164 expression is seen in the
280 glomerulus of the developing renal corpuscle (A.V, B.V, C.V), and weakly in the matured
281 renal corpuscle (A.VI, B.VI, C.VI). In murine kidney *Cep164* expression is seen in the
282 developing renal vesicles (D.II) and ubiquitously throughout subsequent nephron renal
283 tubules (D.IV, EIII, F.IV). *Cep164* expression is seen in the glomerulus of the developing
284 renal corpuscle (D.V), but expression is lost with maturity (D.VI, F.IV). All scale bars
285 represent 100μm.

Cap mesenchyme (CM), collecting duct (CD), distal tubule (DT), loop of henle (LH), postnatal day (P), post conception weeks (PCW), proximal tubule (PT), renal corpuscle (RC), renal tubule (RT), renal vesicle (RV), s-shaped body (SSB), uteric bud (UB).

In the developing human kidney, CEP164 is expressed in the glomerulus of the renal corpuscle at 8 PCW-18 PCW, indicating podocyte CEP164 expression (**Figure 1A.V.VI, B.V.VI, C.V.VI**). The data suggests that CEP164 expression is reduced as the glomeruli matures; this is most clearly seen at 18 PCW.

The human embryonic/foetal renal uteric bud, which forms the collecting duct, is derived from the metanephrogenic diverticulum. Both the uteric bud and collecting duct also show CEP164 expression in the apical membrane of the epithelial cells lining the tubular lumen (8PCW-18PCW) (**Figure 1A.III.VII, B.III.VII, C.III.VII)**. CEP164 is also expressed at the basolateral membrane of the collecting duct tubule (8PCW-18PCW). CEP164 expression is not present in the human renal interstitium (**Figure 1A-C**). Negative control staining indicating that CEP164 expression in the human kidney was specific (**S4 Figure A,B**).

In the murine kidney (*129/OlaHsd-Cep164$^{tm1a(EUCOMM)Wtsi/+}$),* the *LacZ* reporter assay demonstrates that *Cep164* expression correlates with human kidney CEP164 expression. Correspondingly, *Cep164* is expressed in the developing murine renal vesicles, s-shaped bodies (P1.5) (**Figure 1D.I.II**) and the subsequent renal tubules, including nephron segments

in both the cortex and medulla (P29.5) (**Figure 1D.IV, E.I.III.IV**). The staining indicates that there is potentially cell-specific expression within each of the tubular segments. *Cep164* is also expressed in the glomeruli of the renal corpuscle at P1.5, which is not present in mature glomeruli at P29.5 (**Figure 1D.V.VI, E.II**). Likewise, *Cep164* is expressed in the developing mesonephric uteric bud and collecting ducts (**Figure 1D.II**). Controls demonstrate that there is no endogenous *LacZ* expression in the kidney (**S5 Figure B**).

CEP164 expression during human and murine retinal development

In the developing human retina, CEP164 expression is widespread yet defined (**Figure 2A**). In early retinal development (11 PCW) CEP164 is expressed weakly in the developing nerve fibre layer (NFL) (fibrous extensions from the optic nerve) and nerve fibres in the differentiating ganglion cell layer (GCL)/inner plexiform layer (IPL) (**Figure 2A.I**). The basally located layer of cone precursors, which has differentiated from the outer neuroblastic cell layer (ONBL), also demonstrates strong CEP164 expression (**Figure 2A.I**). By 14 PCW, CEP164 expression is defined to the NFL, the IPL and the photoreceptor layer which now has both developing rods and cones (**Figure 2A.II**). Later in development, 19 PCW, once all of the primitive retinal layers have formed, CEP164 expression is maintained in the nerve fibres of the NFL, the ganglionic and inner nuclear nerve fibril synapses of the IPL, and the inner segments (IS) and outer segments (OS) of the photoreceptor cell layer (**Figure 2A.III**). At 19 PCW, CEP164 expression is also present in the developing outer plexiform layer (OPL) which contains nerve fibril synapses between the inner nuclear layer (INL) and the outer nuclear layer (ONL). CEP164 expression in the retinal pigment epithelial layer (RPE) cannot be defined due to its natural dark colouring.

Figure 2. CEP164 expression in the developing human and murine retina

(A) Human Retina, (A.I) 11 PCW, (A.II) 14 PCW, and (A.III) 19 PCW. (B) Murine Retina, (B.I) P1.5, (B.II) P15.5, (B.111) P29.5. In the developing human retina, weak CEP164 expression is seen in the nerve fibre layer (NFL) and ganglion cell layer/inner plexiform layer (GCL/IPL) (A.I) and strong expression in outer neuroblastic (ONBL) photoreceptor precursors (black arrow) (A.1). By 11 PCW, CEP164 expression is seen in the developed inner plexiform layer (IPL) and the developing photoreceptor layers (A.II). At 19 PCW, CEP164 expression is seen in the nerve fibre layer (NFL), inner plexiform layer (IPL), outer plexiform layer (OPL) and photoreceptor layer, with enhancement in the inner photoreceptor segments (IS) (A.III). In the developing murine retina (B), *Cep164* expression is seen in the inner plexiform layer (IPL), ganglion cell layer (GCL) and outer neuroblastic (ONBL) photoreceptor precursors (see arrow) (B.I). At P15.5, *Cep164* expression is seen in the ganglion cell layer (GCL), the outer plexiform layer (OPL) and inner segment (IS) of the photoreceptor layer (B.II). There is also punctate expression in the inner plexiform layer (IPL) and edges of the nuclear cell layers (B.II). Retinal pigment epithelium (RPE) also shows *Cep164* expression (B.I, B.II). This murine retinal expression patterning is maintained after retinal development (B.III).

Ganglion cell layer (GCL), inner nuclear layer (INL), inner plexiform layer (IPL), inner segment (IS), nerve fibre layer (NFL), outer neuroblastic cell layer (ONBL), outer nuclear layer (ONL), outer plexiform layer (OPL), outer segment (OS), photoreceptor segment layer (PS), retinal pigment epithelium (RPE).

Murine *Cep164* retinal expression in (*129/OlaHsd-Cep164$^{tm1a(EUCOMM)Wtsi/+}$* largely corresponds to the human CEP164 expression patterns, with expression maintained in the developing IPL, OPL and PS layer (P1.5-P29.5) (**Figure 2B**). However, there are some clear differences. *Cep164* is expressed in retinal precursor cells throughout the murine ONBL, which in the developing human retina is restricted to the cone precursor cells. Additionally, strong *Cep164* expression is present and maintained throughout the GCL (P1.5-P29.5) (**Figure 2B)**. *Cep164* is also expressed sparsely in some cells of the INL and ONL, however these tend to be at the boundaries of the plexiform layers (P15.5-P29.5) (**Figure 2B.II.III)**. Notably, at later stages of development, *Cep164* expression is clearly defined to the IS of the photoreceptor cell layer (P15.5-P29.5) (**Figure 2B.II.III)**. Additionally, the retinal pigment epithelial layer demonstrates strong, cell-specific *Cep164* expression throughout development (P1.5-P29.5) (**Figure 2B)**. WT controls demonstrate no endogenous X-Gal staining (**S5 Figure A**).

CEP164 expression during human and murine neuronal and cerebellar development

CEP164 is expressed widely throughout human brain development (8PCW-18PCW) (**Figure 3A-D**). At 8PCW CEP164 is strongly expressed in the neuroepithelium of the developing telencephalon (Tel), which is defined in cells lining the lateral ventricle (LV), including the ventricular layer (VL), subventricular layer (SVL), cortical plate (CorP) and marginal layer (MaL), (**Figure 3A.I.VI, B.I.VI**). At 8 PCW, CEP164 is also present in the developing neuroepithelium of the diencephalon (Di), mesencephalon (Mes), metencephalon (Met) and myencephalon (Mye), with expression strongest in the apical epithelium lining the brain ventricles (**Figure 3A.I.V.VI.VII, 3B.I.VI.VII.VIII**). At 8PCW there is strong, well-defined CEP164 expression in the midline of the myencephalon (**Figure 3B.IV.V**), as well as cells of

the nasal epithelium (**Figure 3B.IX**). Throughout human brain development (8PCW-18PCW) the choroid plexus demonstrates strong CEP164 expression, specifically in the ependymal cells, and more weakly in the choroid plexus pia matter **(Figure 3A.II.III.IV, B.II.III, C.V, D.V)**. The developing human cerebellar folds show defined CEP164 expression in the migrating molecular cell layer at 16 PCW, but this is reduced by 18PCW (**Figure 3C.I.II, D.I.II**). CEP164 is expressed at the apical membrane of the ventricular surface of the pons and cerebellum, as well as the myencephalon, specifically in the axon tracts of the medulla oblongata (**Figure 3A.VII.VIII, C.III.IV.VI, D.III.IV.VI**). This expression pattern can be seen from 8PCW to 18 PCW, however CEP164 expression levels are much weaker by 18 PCW. At 8PCW CEP164 is expressed in the white matter, but this is lost with maturation of the cerebellum (**Figure 3A.VII, C.VII, D.VII**). Notably the human foetal brain negative controls demonstrate no positive staining (**S4 Figure D-F**). A PAX6 antibody was used as a positive control (**S4 Figure E,F**).

Figure 3. CEP164 expression in the developing human and murine hindbrain

Developing human hindbrain (A-D), 8 PCW (A-B), 16 PCW (C) and 18 PCW (D).
At 8 PCW in the developing human brain CEP164 expression is seen in the neuroepithelium surrounding the telencephalon, diencephalon, mesencephalon, metencephalon and myencephalon, with defined expression in apical neuroepithelial cells lining the brain ventricles (A.I.V.VI.VII.VIII, BI.VI.VII.VIII) demonstrated by black arrows. Defined expression is present in the layers of the telencephalon (A.VI, B.VI). The choroid plexus shows strong CEP164 expression in the ependymal cells (A.II.III.IV, B.II.III), with weaker expression in the choroid plexus pia matter (A.IV, B.II.III). There is defined expression of CEP164 to the human brain midline (B.IV.V) and the nasal epithelium (B.IX). Choroid plexus ependymal cell expression pattern of CEP164 is maintained (C.I.V, D.I.V). CEP164

407 expression is seen in the migrating molecular cell layer of the developing cerebellum
408 (C.II),which is lost with molecular cell layer maturation (D.II). In the human hindbrain the
409 apical membrane of the pons and the cerebellum demonstrate defined CEP164 expression is
410 seen (C.III,IV), which is lost with maturation (D.II.IV). Weak CEP164 expression is seen in
411 the human medulla oblongata (C.VI, D.VI) but not in the white matter (C.VII, D.VII).
412
413 Developing murine hindbrain (E-H), P0.5 (E-F), P15.5 (G) and P30.5 (H).
414 *Cep164* expression is seen in the developing P0.5 murine brain (E, G.I, H.I) with expression
415 in the cortex, striatum and cerebrum of the maturing cerebral cortex (G.V, H.V), thalamus
416 (G.VI) and midbrain (G.VII, H.VI) at P15.5 and P30.5. *Cep164* expression is strong and
417 defined in the ventricular neuroepithelium (G.VII.VIII). The murine choroid plexus
418 demonstrates strong *Cep164* expression, however it is not defined to a specific cell type.
419 (E.III, F.IV). In the murine model, *Cep164* is expressed in the migrating molecular layer
420 (FI.II), however this expression is maintained throughout development with expression also
421 in the molecular layer, ganglion cell layer and Purkinje cell layer (G.III,H.III). *Cep164*
422 expression is seen in the murine cerebellum (F.III,G.III), in the murine pons (F.V, H.VI), and
423 weakly in the cerebellar white matter (F.VI), which is lost with maturation (H.IV).
424
425 Aquaduct (Aq), axon tract (AT), cerebellum (Ce), cerebral cortex (CC), cerebral hemisphere
426 (CH), cerebrum (Cr), choroid plexus (CP), cortex (Cor), cortical plate (CorP), diencephalon
427 (Di), ependymal cells (Ep), fourth ventricle (FV), ganglion cell layer (GCL), inner plexiform
428 layer (IPL), intermediate zone (IL), lateral ventricle (LV), marginal layer (MaL), medulla
429 oblongata (MO), mesencephalon (Mes), metencephalon (Met), midbrain (MB), midline (Mi),
430 molecular cell layer (MCL), myencephalon (Mye), nasal epithelium (Na), outer neuroblastic
431 layer (ONBL), pia (P), pons (PO), purkinje cell layer (PCL), retinal pigment epithelium

(RPE), striatum (St), sub-ventricular layer (SVL), telencephalon (Tel), thalamus (Th), third ventricle (TV), ventricular layer (VL), ventricular surface (VS), white matter (WM).

Corresponding with the developing human brain, *Cep164* is expressed in the neuroepithelium of the murine telencephalon (*129/OlaHsd-Cep164$^{tm1a(EUCOMM)Wtsi/+}$*) (cerebral hemisphere), diencephalon, mesencephalon (midbrain), metencephalon (pons) and myencephalon (medulla oblongata) at P0.5 (**Figure 3E.I.VI.VII.VIII, F.V**). At later stages of development (P15.5-P30.5), clear *Cep164* expression can be seen throughout the brain including the cerebrum and striatum of the cerebral cortex, the thalamus of the diencephalon, the midbrain and hindbrain pons and medulla oblongata (**Figure 3G.I.V.VI.VII.VIII, H.I.V.VI.VII**). Additionally, correlating with human foetal expression, *Cep164* is expressed strongly in neuroepithelium lining the brain ventricles, including the third ventricle, fourth ventricle and cerebral aquaduct (**Figure 3G.VI.VII**).

At P0.5 to P15.5 *Cep164* is expressed in the migrating molecular cell layer and Purkinje layer of the cerebellum (**Figure 3F.I.II, G.I.II.III).** Later in development, *Cep164* is also expressed in the ganglion cell layer (P30.5) (**Figure 3H.I.II.III**), potentially this might be seen later on in human foetal development. *Cep164* is also expressed at the apical membrane of the ventricular surface of the cerebellum at P0.5 and P15.5 (**Figure 3F.III, G.III**). Unlike the human cerebellar expression, *Cep164* is expressed in the white matter of the cerebellum which is present, although reduced at P30.5 (**Figure 3E.IV, F.VI, G.IV, H.IV**). *Cep164* is also expressed in the choroid plexus, ependymal cells, which is demonstrated in P0.5 sections (**Figure 3E.I.II.III, F.IV**). Murine controls demonstrate that there is no endogenous *LacZ* expression in the murine brain (**S5 Figure F-H**).

CEP164 expression during human and murine development in other tissues

CEP164 is expressed widely throughout the developing human embryo at 8PCW (**Figure 4A.I**.). In the 8PCW lung, CEP164 is expressed most strongly in the epithelial cells lining the lumen of the bronchi and bronchioles (**Figure 4A.II.III**). Weaker CEP164 expression is also present in the bronchiole smooth muscle, and the alveoli primordia (**Figure 4A.II.III**). In the 8PCW developing heart, CEP164 is expressed in cardiomyocytes (**Figure 4A.IV.V**). The gastrointestinal tract also shows strong defined CEP164 expression in the inner mucosa squamous epithelium cell layer, muscularis mucosae cell layer and the external muscularis externa layer at 8PCW (**Figure 4A.VI**). At 8PCW in the developing gonads, CEP164 is expressed weakly in the germline epithelium, but strongly in the seminiferous cord tubules (**Figure 4A.VII.VIII**). Additionally, CEP164 is expressed strongly in the dorsal root ganglia of the spinal cord, with weak expression in the developing vertebrae (**Figure 4A.X**). CEP164 is also expressed in developing bone primordia of the limbs at 8 PCW (**Figure 4A.X**).

Figure 4. CEP164 expression in secondary organs throughout human and murine development

(A) Human 8 PCW. (B) Murine; P0.5 (B.I-III), P15.5 (B.IV-XVII), P30.5 (C.I-IXV). In the developing human, lung CEP164 expression is seen in the respiratory epithelial lining of the bronchi and bronchioles, with weaker expression in the smooth muscle and alveoli (AII.III). In the developing murine lung, Cep164 expression is in respiratory epithelial lining of the bronchi and bronchioles, with additional *Cep164* expression seen in the respiratory epithelial cells lining the trachea and the tertiary bronchioles (B.IV.V.VI.VII.VIII.IX, C.I.IV.V.VI). *Cep164* is expression is seen in murine alveoli (B.IX), which is lost with maturity (B.VII).

480 *Cep164* expression is seen within the cartilage of the trachea (B.V.VI, C.II.III). In the human
481 heart, CEP164 expression is seen in the developing cardiomyocytes (A.IV.V). In the murine
482 heart Cep164 expression is seen in the developing cardiomyocytes (B.X.XI, C.VIII,IX). In
483 the human gastrointestinal tract CEP164 expression is seen in the inner mucosae squamous
484 epithelial cell layer, muscularis mucosae cell layer and the external muscularis cell layer
485 (A.VII). In the developing human gonads, CEP164 expression is seen in the germline
486 epithelium and seminiferous cord (A.VII.VIII). In the developing murine testes, P15.5,
487 *Cep164* expression is seen in the seminiferous tubules, specifically the smooth muscle cells
488 spermatogonia, spermatocytes and most strongly in spermatids (B.XI.XII.XIII); expression in
489 leydig cells and connective tissue can also be seen (B.IXX). At P30.5, Cep164 expression is
490 defined to the spermatogonia, spermatocytes and spermatids (C.X.XI.XII).
491 CEP164 expression is seen in the dorsal root ganglia of the human spinal cord, (A.IX) with
492 weaker expression also present in the vertebrae primordia (A.IX) and bone primordia (A.X).
493 *Cep164* expression is seen in the murine developing costal cartilage, with weaker expression
494 in intercostal muscle (B.II.III). The human foetal liver demonstrates some evidence of
495 CEP164 expression (A.XI). The developing murine liver demonstrates *Cep164* expression in
496 epithelial cells lining the hepatic portal veins (B.XV.XVI.XVII, C.XIII.XIV), but no
497 expression is seen in hepatocytes.
498
499 Aveoli (Av), alveoli primordia (Av Pri), bile duct (BD), bone primordia (BP), bronchiole
500 (Br), cardiomyocyte (CM), cartilage (Ca), connective tissue (CT), costal cartilage (CC),
501 dorsal root ganglia (DRG), epithelial (Ep), gastrointestinal tract (GI), germline epithelium
502 (GE), gonad (Go), heart (Ht), hepatocytes (Hep), intercostal muscle (IC), kidney (Ki), lamina
503 propria (LM), liver (Li), lung (Lu), muscularis externa (ME), muscularis mucosae (MM),
504 respiratory bronchiole (R), seminiferous cord (SeC), seminiferous tubule (ST), smooth

505 muscle (SM), spermatids (Sp), spermatocytes (SC), spermatogonia (Spg), squamous cell
506 mucosae (Mc-sq), submucosae (SB), trachea (Tr), terminal bronchi (TB), vertebrae (Vt).
507
508
509

510 Murine postnatal tissues also demonstrate widespread *Cep164* expression. At P0.5 *Cep164* is
511 expressed in the developing costal cartilage primordia and intercostal muscles (**Figure**
512 **4B.I.II.III**). Correlating with the human lung, in the developing murine P15.5 and P30.5
513 lung, *Cep164* is present in the epithelial cells lining the trachea, bronchioles and
514 terminal/respiratory bronchioles, as well as the smooth muscle and cartilage of the trachea
515 and bronchi. (**Figure 4B.IV.V.VII.VIII, C.I.II.III.IV.V.VI**).Weak *Cep164* expression is
516 seen in the alveoli at P15.5, which is reduced by P29.5 (**Figure 4B.IX, C.VII**). Like human
517 embryonic tissues, *Cep164* is present in cardiomyocytes at P15.5 and P30.5 (**Figure**
518 **4B.X.XI, C.VIII.IX**). In postnatal P15.5 murine testes, *Cep164* is expressed in the
519 connecting tubules and Leydig cells **(Figure 4B.XII.XIII.XIV).** In the seminiferous tubules,
520 *Cep164* is expressed in the smooth muscle cells and weakly in developing spermatogonia and
521 spermatocytes. Strong *Cep164* expression is present in the spermatid tails. By P30.5 *Cep164*
522 expression is defined to developing spermatogonia, spermatocytes, and spermatids (**Figure**
523 **4C.X.XI.XII**). At P15.5 and P30.5 *Cep164* is expressed strongly in cells lining the ciliated
524 cholangiocyte cells of the bile duct, however hepatocytes do not show any expression
525 (**Figure 4C.XV.XVI.XVII, D.XIII.XIV**). Wholemount *Cep164* expression studies (E9.5,
526 E10.5, E12.5), demonstrate that *Cep164* expression is widespread throughout murine
527 embryonic development, including the bronchial arches and organ primordia, as well as the
528 developing CNS, heart and limbs (**S3 Figure**). Taken together this indicates that CEP164

529 expression is widespread throughout human and murine development in tissues beyond the
530 cerebello-retinal-renal structures associated with typical disease phenotypes.

531

532 **Discussion**

533 In this study we have described the expression of CEP164 in the developing human embryo
534 and foetus, utilising immunohistochemistry, focusing upon the kidney, retina and cerebellum.
535 Conservation of CEP164 expression was explored using a *LacZ* gene trap assay to
536 characterise *Cep164* expression in corresponding murine tissues (*129/OlaHsd-*
537 *Cep164*$^{tm1a(EUCOMM)Wtsi/+}$). Notably, during murine development, the kidney, retina and
538 cerebellum continue to develop postnatally. This reflects the chosen murine postnatal
539 timepoints in this study, corresponding to estimated human embryonic and fetal
540 developmental timepoints (**S2 Table, S3 Table, S4 Table**).

541

542 Our results demonstrate that during human and murine development CEP164 is expressed
543 widely, in multiple organs. Notably, CEP164 expression is clearly defined within tissues. In
544 the developing human kidney, CEP164 is expressed in the apical epithelium membrane of
545 metanephric-derived renal vesicles and subsequent nephron tubules (8PCW-18PCW),
546 correlating with the presence of primary cilia [37]. Primary cilia are vital in the kidney for
547 mechanosensation and chemical signal transduction, which is required for orientated cellular
548 divisions during development and kidney maintenance. As CEP164 expression seems to be
549 low/not present in the cap mesenchyme, it could be speculated that CEP164 expression is
550 switched on during mesenchymal-epithelial transition, which coincides with the formation of
551 the primary cilium during establishment of apical-basal polarity, cell junctions and lumen
552 formation [37]. CEP164 is expressed within the glomerulus of the renal corpuscle, with a

553 reduction in expression with maturity. Interestingly, this correlates with the loss of primary
554 cilium in podocytes seen with glomeruli maturity in rats [38]. It could be postulated that in
555 the developing human kidney, primary cilium, and thus CEP164 expression, is lost in
556 maturing glomeruli [38]. This could protect against overstimulation of calcium-mediated
557 signalling due to an increase in glomerular filtration rate [38]. CEP164 is also expressed in
558 the uteric bud, which develops into the primary ciliated collecting duct network (8PCW-
559 18PCW), consistent with numerous IMCD3 expression studies [1, 19, 20, 25, 32]. The human
560 CEP164 expression pattern is conserved in the murine kidney (P0.5-P29.5); there may be
561 cell-specific *Cep164* expression within nephron tubular segments, however this would need
562 to be further studied.

563

564 Although our data is focused upon development, the human protein atlas indicates that the
565 CEP164 expression is maintained in the adult kidney [39]. A combination of P30.5
566 expression data and previous wholemount *Cep164* expression studies also indicate that
567 *Cep164* expression is maintained in the adult mouse kidney [36]. Together this suggests that
568 CEP164 may have roles in both normal renal development and maintenance of kidney
569 function in the human and mouse. Aberrant CEP164 function in the kidney could contribute
570 to abnormal primary cilium functioning, causing dysfunctions in cell divisions and cell
571 signalling, leading to cystogenesis. This is consistent with the NPHP-RC phenotype present
572 in most patients with *CEP164* mutations [1].

573

574 In the human retina, CEP164 is expressed in the NFL, OPL, IPL and photoreceptor layer
575 between 8PCW-18PCW. CEP164 expression in the GCL is lost prior to 14 PCW, whereas it
576 is maintained in the murine retina (P0.5-P29.5). The murine retina also shows *Cep164*

577 expression in the ONBL primordial layer, with punctuate expression at the edges of the INL
578 and ONL. Multiple studies have suggested that primary cilia are present and functional in
579 neurones [40]. It could be speculated they are also present in the neurones seen in the NFL,
580 OPL, IPL, GCL, ONBL, IBL and OBL, which would link with CEP164 expression. The
581 human and murine retina have shown some differences in gene and protein expression in
582 previous studies, potentially this is the case with CEP164 in the retina [41].

583

584 Retinal photoreceptor cells have a specialised connecting primary cilium between the inner
585 and outer segment of the photoreceptors. It therefore seems reasonable that CEP164, a distal
586 appendage centrosomal protein, is expressed in photoreceptor segment in the developing
587 human and murine retina. CEP164 expression has been previously identified in the murine
588 connecting cilium, further confirming our results [1, 42].

589

590 In the murine retina, C*ep164* expression is defined to the inner segment of the photoreceptor
591 layer by P15.5. This correlates with previous preliminary *Cep164 In Situ hybridisation*
592 studies [43]. It can be hypothesised that the *Cep164* is transcribed and translated in the inner
593 segment but then the CEP164 protein is transported to the outer segment of the photoreceptor
594 cells; this would not be detected by the X-Gal assay but could be defined in the human assay.
595 Interestingly, the murine *Cep164* expression pattern is maintained in the adult mouse. It is
596 likely that human CEP164 expression is also maintained in the human adult retina, potentially
597 with a role in retinal development and tissue functioning.

598 It is also well established that CEP164 is present at the basal body of retinal pigment
599 epithelial cells, clarifying the results from our study [1, 2, 15, 17, 23]. It can be hypothesised
600 that with abnormal functioning/loss of CEP164, there could be atypical outer segment

601 formation, which could lead to the accumulation of phototransduction proteins that could
602 trigger cell loss, leading to a retinal degeneration phenotype, as seen in some *CEP164*
603 NPHP-RC patients [1, 9, 44].

604

605 CEP164 is expressed throughout the developing human brain (8PCW-18PCW) and the
606 developing murine brain (P0.5-P29.5), including the telencephalon, diencephalon,
607 mesencephalon, metencephalon and myencephalon. In early human development (8 PCW)
608 CEP164 is expressed widely throughout the cerebellum, including the white matter. By 16
609 PCW this expression is focused to the migrating molecular cell layer, however CEP164
610 expression is still strong in the axon tracts of the medulla oblongata and the apical
611 neuroepithelium membrane surrounding the pons and cerebellum. At 18 PCW CEP164
612 staining in the molecular layer is considerably weaker. Human protein atlas studies indicate
613 that CEP164 is present at low levels within the cerebral cortex, hippocampus and caudate, but
614 is not expressed within the adult cerebellum, however these studies have not been validated
615 [39].

616

617 Primary cilia are vital in the developing brain for Shh signalling, which is needed for
618 proliferation of neuronal granular cell precursors in vertebrates, being a major driver of
619 cerebellar precursors [45, 46]. Shh is also required for the cell-specific expansion of postnatal
620 progenitors [40]. Wnt signalling, transduced by the primary cilia, is also required for neuronal
621 patterning, cell proliferation and neuronal migration [46-48]. In the adult nervous system,
622 primary cilia are thought to be required in stem cell regulation and tissue regeneration,
623 however the full extent of primary cilia function in the adult central nervous system is still to
624 be determined [40, 45]. It could be suggested that CEP164 has a functional role in human

625 brain development. Potentially, aberrant function of CEP164, may lead to brain dysplasia via
626 abnormal primary cilia functioning in neuronal precursors. Some CEP164 NPHP-RC
627 patients show neurological phenotypes, including abnormal developmental delay, intellectual
628 disability and in one patient, cerebellar vermis aplasia, an archetypal feature of Joubert
629 syndrome. Another patient also experiences seizures [1, 9].

630

631 In the murine cerebellum, *Cep164* expression is widespread including the migrating
632 molecular, ganglion and Purkinje cell layers, as well as the white matter (P0.5-P29.5).
633 Wholemount expression studies from the international phenotyping consortium have shown
634 that *Cep164* is expressed strongly throughout the adult murine brain [36]. It may be that
635 *Cep164* RNA expression does not directly correlate with CEP164 protein expression.
636 Although there is believed to be high conservation between the human and murine
637 transcriptomic networks, CEP164 may be part of the divergent pathway in the human-murine
638 brain transcriptomics [46].

639

640 Leptin receptors are situated in the primary cilia on the choroid plexus, and in the
641 hypothalamus [47]. Leptin signalling is vital in the hypothalamic satiety pathway. Patients
642 with mutations in centrosomal BBS proteins demonstrate hyperleptinemia due to leptin
643 resistance, which causes hyperphagia and subsequent weight gain. It could be hypothesised
644 that CEP164, which is expressed in the developing choroid plexus of the human (8 PCW, 16
645 PCW, 18PCW) and murine brain (P0.5), may not only play a role in gross neurological
646 development, but may also be involved indirectly in leptin receptor localisation or
647 functioning within the primary cilium. This could contribute to the obesity phenotype seen in
648 some CEP164 NPHP-RC patients [1, 9].

649

650 Ependymal cells of the choroid plexus, which contain motile cilia, are required for the
651 production and regulation of cerebral spinal fluid (CSF). Additionally, the lateral ventricle
652 epithelium contains motile cilia which is important for the movement of CSF throughout the
653 brain ventricles. Previous studies have established a ciliogenesis role for CEP164 in the
654 motile cilium and demonstrated CSF defects including hydrocephalus in zebrafish and
655 murine models lacking a functioning CEP164 [24]. This further validates the strong CEP164
656 expression in ependymal cells and the neuroepithelium lining the brain ventricles.

657

658 CEP164 is also expressed in tissues secondary to the cerebellar-retinal-renal phenotype, some
659 of which have motile cilium. Taking together results from a previous murine CEP164 motile
660 cilia study [24], it is plausible that CEP164 is expressed in the ciliated epithelial cells of the
661 trachea, bronchi and bronchioles in the human (8 PCW) and murine (P15.5-P29.5) lung.
662 Previous studies indicate that this is likely to be maintained in the adult human and murine
663 lung [36, 39]. *Cep164* is also expressed in the murine spermatids, which have a flagellum,
664 effectively a modified motile cilium [48]. Studies have demonstrated that CEP164 is
665 expressed in the capitulum and striated columns of the human sperm neck [49]. Using
666 information from a recent FOXJ1 mediated knockout of *Cep164,* it could be hypothesised
667 that CEP164 is required for the formation, maintenance and functioning of motile cilia within
668 the respiratory epithelium, reproductive tissues and the sperm flagella [24]. Mutations and
669 subsequent aberrant functioning or loss of CEP164 may contribute to lung phenotypes such
670 as pulmonary bronchiectasis, as seen in some patients with *CEP164* mutations [1]. This may
671 also contribute to aberrant spermatid function, which may cause infertility problems as seen
672 typically in BBS models [9].

673

674 CEP164 is also expressed in other developing tissues that contain a primary cilium, (human 8
675 PCW, mouse P15.5-30.5); including cardiomyocytes of the heart, cholangiocytes of the liver
676 bile ducts, smooth muscle cells, cartilage, spermatogonia and spermatocytes, bone primordia
677 and the epithelium lining and smooth muscles of the GI tract [50-57]. Accordingly, CEP164
678 is not present in the hepatocytes, which do not contain primary cilium [58].

679

680 CEP164 is expressed in tissues involved in the CEP164 NPHP-RC phenotype, but is also
681 expressed in tissues not associated with this phenotype. It could be that CEP164 has cell-
682 specific functions, not all tissues may rely on the primary cilium for development or have
683 other pathways that can compensate for the abnormal functioning or loss of CEP164.
684 Remarkably, human CEP164 expression patterns demonstrated here correlate with previously
685 reported expression patterns of the JBTS genes *AHI1* and *CEP290* [59]. This could indicate a
686 universal mechanism that underlies NPHP-RC.

687

688 In summary, CEP164 demonstrates widespread yet defined expression throughout human and
689 murine development, which is predominantly maintained into adult life. Human and murine
690 data largely correlate and CEP164 function is likely to be conserved between the two species.
691 CEP164 is expressed in tissues affected in CEP164-NPHP-RC patients, however clinical
692 heterogeneity, commonly seen in ciliopathies, needs to be further investigated.

693

694

695 **Acknowledgements**

696 L.A.D is funded by the Medical Research Council Discovery Medicine North Doctoral

697 Training Partnership, and The Northern Counties Kidney Research Fund.

698

699

700

701

702

703

References

1. Chaki, M., et al., *Exome capture reveals ZNF423 and CEP164 mutations, linking renal ciliopathies to DNA damage response signaling.* Cell, 2012. **150**(3): p. 533-48.
2. Graser, S., et al., *Cep164, a novel centriole appendage protein required for primary cilium formation.* J Cell Biol, 2007. **179**(2): p. 321-30.
3. Utsch, B., et al., *Identification of the first AHI1 gene mutations in nephronophthisis-associated Joubert syndrome.* Pediatr Nephrol, 2006. **21**(1): p. 32-5.
4. Delous, M., et al., *The ciliary gene RPGRIP1L is mutated in cerebello-oculo-renal syndrome (Joubert syndrome type B) and Meckel syndrome.* Nat Genet, 2007. **39**(7): p. 875-81.
5. Maria, B.L., et al., *"Joubert syndrome" revisited: key ocular motor signs with magnetic resonance imaging correlation.* J Child Neurol, 1997. **12**(7): p. 423-30.
6. Lambert, S.R., et al., *Joubert syndrome.* Arch Ophthalmol, 1989. **107**(5): p. 709-13.
7. Sturm, V., et al., *Ophthalmological findings in Joubert syndrome.* Eye (Lond), 2010. **24**(2): p. 222-5.
8. van Dorp, D.B., et al., *Joubert syndrome: a clinical and pathological description of an affected male and a female fetus from the same sibship.* Am J Med Genet, 1991. **40**(1): p. 100-4.
9. Maria, M., et al., *Genetic and clinical characterization of Pakistani families with Bardet-Biedl syndrome extends the genetic and phenotypic spectrum.* Sci Rep, 2016. **6**: p. 34764.
10. Parisi, M.A., et al., *Joubert syndrome (and related disorders) (OMIM 213300).* Eur J Hum Genet, 2007. **15**(5): p. 511-21.
11. Brancati, F., B. Dallapiccola, and E.M. Valente, *Joubert Syndrome and related disorders.* Orphanet J Rare Dis, 2010. **5**: p. 20.
12. Srivastava, S., et al., *Many Genes-One Disease? Genetics of Nephronophthisis (NPHP) and NPHP-Associated Disorders.* Front Pediatr, 2017. **5**: p. 287.
13. Kikuno, R., et al., *Prediction of the coding sequences of unidentified human genes. XIV. The complete sequences of 100 new cDNA clones from brain which code for large proteins in vitro.* DNA Res, 1999. **6**(3): p. 197-205.
14. Sivasubramaniam, S., et al., *Cep164 is a mediator protein required for the maintenance of genomic stability through modulation of MDC1, RPA, and CHK1.* Genes Dev, 2008. **22**(5): p. 587-600.
15. Schmidt, K.N., et al., *Cep164 mediates vesicular docking to the mother centriole during early steps of ciliogenesis.* J Cell Biol, 2012. **199**(7): p. 1083-101.
16. Andersen, J.S., et al., *Proteomic characterization of the human centrosome by protein correlation profiling.* Nature, 2003. **426**(6966): p. 570-4.
17. Daly, O.M., et al., *CEP164-null cells generated by genome editing show a ciliation defect with intact DNA repair capacity.* J Cell Sci, 2016. **129**(9): p. 1769-74.
18. Sonnen, K.F., et al., *3D-structured illumination microscopy provides novel insight into architecture of human centrosomes.* Biol Open, 2012. **1**(10): p. 965-76.
19. Lau, L., et al., *STED microscopy with optimized labeling density reveals 9-fold arrangement of a centriole protein.* Biophys J, 2012. **102**(12): p. 2926-35.
20. Shi, X., et al., *Super-resolution microscopy reveals that disruption of ciliary transition-zone architecture causes Joubert syndrome.* Nat Cell Biol, 2017. **19**(10): p. 1178-1188.
21. Sillibourne, J.E., et al., *Assessing the localization of centrosomal proteins by PALM/STORM nanoscopy.* Cytoskeleton (Hoboken), 2011. **68**(11): p. 619-27.
22. Yang, *Super-resolution architecture of mammalian centriole distal appendages reveals distinct blade and matrix functional components.* Nature Communications, 2018(9).
23. Tanos, B.E., et al., *Centriole distal appendages promote membrane docking, leading to cilia initiation.* Genes Dev, 2013. **27**(2): p. 163-8.
24. Siller, S.S., et al., *Conditional knockout mice for the distal appendage protein CEP164 reveal its essential roles in airway multiciliated cell differentiation.* PLoS Genet, 2017. **13**(12): p. e1007128.

25. Slaats, G.G., et al., *Nephronophthisis-associated CEP164 regulates cell cycle progression, apoptosis and epithelial-to-mesenchymal transition.* PLoS Genet, 2014. **10**(10): p. e1004594.
26. Kong, D., et al., *Centriole maturation requires regulated Plk1 activity during two consecutive cell cycles.* J Cell Biol, 2014. **206**(7): p. 855-65.
27. Slaats, G.G., et al., *DNA replication stress underlies renal phenotypes in CEP290-associated Joubert syndrome.* Journal of Clinical Investigation, 2015. **125**(9): p. 3657-3666.
28. Humbert, M.C., et al., *ARL13B, PDE6D, and CEP164 form a functional network for INPP5E ciliary targeting.* Proc Natl Acad Sci U S A, 2012. **109**(48): p. 19691-6.
29. Cajanek, L. and E.A. Nigg, *Cep164 triggers ciliogenesis by recruiting Tau tubulin kinase 2 to the mother centriole.* Proc Natl Acad Sci U S A, 2014. **111**(28): p. E2841-50.
30. Burke, M.C., et al., *Chibby promotes ciliary vesicle formation and basal body docking during airway cell differentiation.* J Cell Biol, 2014. **207**(1): p. 123-37.
31. Goetz, S.C. and K.V. Anderson, *The primary cilium: a signalling centre during vertebrate development.* Nat Rev Genet, 2010. **11**(5): p. 331-44.
32. Oda, T., et al., *Binding to Cep164, but not EB1, is essential for centriolar localization of TTBK2 and its function in ciliogenesis.* Genes Cells, 2014. **19**(12): p. 927-40.
33. Pan, Y.R. and E.Y. Lee, *UV-dependent interaction between Cep164 and XPA mediates localization of Cep164 at sites of DNA damage and UV sensitivity.* Cell Cycle, 2009. **8**(4): p. 655-64.
34. Ensembl. *Cep164 Murine*. 2018; Available from: http://www.ensembl.org/Mus_musculus/Gene/Summary?db=coreg=ENSMUSG00000043987r=9:45766946-45828691.
35. UCSC. *Cep164*. 2018; Available from: https://genome-euro.ucsc.edu/cgi-bin/hgTracks?db=mm10&lastVirtModeType=default&lastVirtModeExtraState=&virtModeType=default&virtMode=0&nonVirtPosition=&position=chr9%3A45766946%2D45828638&hgsid=228133814_F2CW3i2YqX1AWfv9drbXnDClGq0v.
36. IMPC. *Cep164*. 2018; Available from: http://www.mousephenotype.org/data/genes/MGI:2384878.
37. Saraga-Babic, M., et al., *Ciliogenesis in normal human kidney development and post-natal life.* Pediatr Nephrol, 2012. **27**(1): p. 55-63.
38. Ichimura, K., H. Kurihara, and T. Sakai, *Primary cilia disappear in rat podocytes during glomerular development.* Cell Tissue Res, 2010. **341**(1): p. 197-209.
39. Atlas, T.H.P. *CEP164*. 2018; Available from: http://www.proteinatlas.org/search/cep164.
40. Fuchs, J.L. and H.D. Schwark, *Neuronal primary cilia: a review.* Cell Biol Int, 2004. **28**(2): p. 111-8.
41. Bibb, L.C., et al., *Temporal and spatial expression patterns of the CRX transcription factor and its downstream targets. Critical differences during human and mouse eye development.* Hum Mol Genet, 2001. **10**(15): p. 1571-9.
42. Liu, Q., et al., *The proteome of the mouse photoreceptor sensory cilium complex.* Mol Cell Proteomics, 2007. **6**(8): p. 1299-317.
43. Blackshaw, S., et al., *Genomic analysis of mouse retinal development.* PLoS Biol, 2004. **2**(9): p. E247.
44. Westlake, C.J., et al., *Primary cilia membrane assembly is initiated by Rab11 and transport protein particle II (TRAPPII) complex-dependent trafficking of Rabin8 to the centrosome.* Proc Natl Acad Sci U S A, 2011. **108**(7): p. 2759-64.
45. Guemez-Gamboa, A., N.G. Coufal, and J.G. Gleeson, *Primary cilia in the developing and mature brain.* Neuron, 2014. **82**(3): p. 511-21.
46. Miller, J.A.H., S, Geshwind. D.H. , *Divergence of human and mouse brain transcriptome highlights Alzheimer disease pathways.* . PNAS, 2009. **107**(28): p. 12698-12703.
47. Lynn, R.B., et al., *Autoradiographic localization of leptin binding in the choroid plexus of ob/ob and db/db mice.* Biochem Biophys Res Commun, 1996. **219**(3): p. 884-9.
48. Afzelius, B.A., *Cilia-related diseases.* J Pathol, 2004. **204**(4): p. 470-7.
49. Fishman, E.L., et al., *A novel atypical sperm centriole is functional during human fertilization.* Nat Commun, 2018. **9**(1): p. 2210.

50. Clement, C.A., et al., *The primary cilium coordinates early cardiogenesis and hedgehog signaling in cardiomyocyte differentiation.* J Cell Sci, 2009. **122**(Pt 17): p. 3070-82.
51. Koefoed, K., et al., *Cilia and coordination of signaling networks during heart development.* Organogenesis, 2014. **10**(1): p. 108-25.
52. Saqui-Salces, M., et al., *A high-fat diet regulates gastrin and acid secretion through primary cilia.* FASEB J, 2012. **26**(8): p. 3127-39.
53. McGlashan, S.R., C.G. Jensen, and C.A. Poole, *Localization of extracellular matrix receptors on the chondrocyte primary cilium.* J Histochem Cytochem, 2006. **54**(9): p. 1005-14.
54. Delaine-Smith, R.M., A. Sittichokechaiwut, and G.C. Reilly, *Primary cilia respond to fluid shear stress and mediate flow-induced calcium deposition in osteoblasts.* FASEB J, 2014. **28**(1): p. 430-9.
55. Temiyasathit, S. and C.R. Jacobs, *Osteocyte primary cilium and its role in bone mechanotransduction.* Ann N Y Acad Sci, 2010. **1192**: p. 422-8.
56. Best, J., et al., *Role of liver progenitors in liver regeneration.* Hepatobiliary Surg Nutr, 2015. **4**(1): p. 48-58.
57. Masyuk, A.I., T.V. Masyuk, and N.F. LaRusso, *Cholangiocyte primary cilia in liver health and disease.* Dev Dyn, 2008. **237**(8): p. 2007-12.
58. Clotman, F., et al., *Lack of cilia and differentiation defects in the liver of human foetuses with the Meckel syndrome.* Liver Int, 2008. **28**(3): p. 377-84.
59. Hynes, A.M., et al., *Murine Joubert syndrome reveals Hedgehog signaling defects as a potential therapeutic target for nephronophthisis.* Proceedings of the National Academy of Sciences of the United States of America, 2014. **111**(27): p. 9893-9898.
60. Chauvet, V., et al., *Expression of PKD1 and PKD2 transcripts and proteins in human embryo and during normal kidney development.* Am J Pathol, 2002. **160**(3): p. 973-83.
61. Seely, J.C., *A brief review of kidney development, maturation, developmental abnormalities, and drug toxicity: juvenile animal relevancy.* J Toxicol Pathol, 2017. **30**(2): p. 125-133.
62. Faa, G., et al., *Morphogenesis and molecular mechanisms involved in human kidney development.* J Cell Physiol, 2012. **227**(3): p. 1257-68.
63. Lindstrom, N.O., et al., *Conserved and Divergent Features of Human and Mouse Kidney Organogenesis.* J Am Soc Nephrol, 2018. **29**(3): p. 785-805.
64. Little, M.H. and A.P. McMahon, *Mammalian kidney development: principles, progress, and projections.* Cold Spring Harb Perspect Biol, 2012. **4**(5).
65. Cheng, Y.Z., et al., *Investigating Embryonic Expression Patterns and Evolution of AHI1 and CEP290 Genes, Implicated in Joubert Syndrome.* Plos One, 2012. **7**(9).
66. Davidson, A.J., *Mouse kidney development*, in *StemBook*. 2008: Cambridge (MA).
67. Wu, B., D. Sahoo, and J.D. Brooks, *Comprehensive gene expression changes associated with mouse postnatal kidney development.* J Urol, 2013. **189**(6): p. 2385-90.
68. Al-Jaberi, N., et al., *The early fetal development of human neocortical GABAergic interneurons.* Cereb Cortex, 2015. **25**(3): p. 631-45.
69. Hill, M.A., *Embryology Vision - Retina Development.* . 2019.
70. Spira, A.W. and M.J. Hollenberg, *Human retinal development: ultrastructure of the inner retinal layers.* Dev Biol, 1973. **31**(1): p. 1-21.
71. Hollenberg, M.J. and A.W. Spira, *Human retinal development: ultrastructure of the outer retina.* Am J Anat, 1973. **137**(4): p. 357-85.
72. Zhang, X., J.M. Serb, and M.H. Greenlee, *Mouse retinal development: a dark horse model for systems biology research.* Bioinform Biol Insights, 2011. **5**: p. 99-113.
73. Zhang, S.S., et al., *A biphasic pattern of gene expression during mouse retina development.* BMC Dev Biol, 2006. **6**: p. 48.
74. Cho, K.H., et al., *Early fetal development of the human cerebellum.* Surg Radiol Anat, 2011. **33**(6): p. 523-30.
75. White, J.J. and R.V. Sillitoe, *Development of the cerebellum: from gene expression patterns to circuit maps.* Wiley Interdiscip Rev Dev Biol, 2013. **2**(1): p. 149-64.
76. Abraham, H., et al., *Cell formation in the cortical layers of the developing human cerebellum.* Int J Dev Neurosci, 2001. **19**(1): p. 53-62.

77. Sudarov, A. and A.L. Joyner, *Cerebellum morphogenesis: the foliation pattern is orchestrated by multi-cellular anchoring centers.* Neural Dev, 2007. **2**: p. 26.
78. Martinez, S., et al., *Cellular and molecular basis of cerebellar development.* Front Neuroanat, 2013. **7**: p. 18.

Supporting Information Captions

S1 Table. Working dilutions of primary antibodies used for immunohistochemistry of human tissues

S2 Table. Comparison of human and murine kidney developmental timeline

S3 Table. Comparison of human and murine retina developmental timeline

S4 Table. Comparison of human and murine cerebellar development timeline

906 **S1 Figure. Conservation and protein domains of human CEP164**

907 (A) Predicted human CEP164 protein domains; tryptophan-tryptophan (WW) domain
908 conserved with two Tryptophan (W) residues, Lysine-rich repeat (LR) and predicted coiled-
909 coil (CC) domains. Values marked are amino acid number. (B) Sequence alignment of human
910 CEP164 and its orthologs *in M.musculus, D.melanogaster, C. reinhardtii* and *D rerio*. (C)
911 Unrooted phylogenetic tree of CEP164 orthologs. (D) Taxonomic profiles of CEP164 derived
912 from EggNOG4.5.1 showing absence of CEP164 in nematoda taxa.

913

914 **S2 Figure. Diagram of the *129/OlaHsd- Cep164^{tm1a}* allele**

915 Upon pre-mRNA splicing of *Cep164^{tm1a}*, exon 3 splices into the splice acceptor (SA) of the
916 *LacZ* cassette, causing a frameshift and subsequent formation of a premature termination
917 codon, this forms the tm1b allele. The *LacZ* has an internal ribosomal entry site (IRES), and
918 thus the *LacZ* fusion gene acts as a reporter gene for *Cep164*.

919

920 Internal ribosomal entry site (IRES), splice acceptor (SA), polyadenylation site (pA).

921

922 **S3 Figure. CEP164 wholemount expression throughout murine embryonic development**
923 **and corresponding WT littermate controls**

924 At E9.5 (A), *Cep164* widespread expression is seen, including the branchial arches,
925 developing forebrain, midbrain and hindbrain (A.I). There is also *Cep164* expression seen in
926 the developing neural tube, including the neuroepithelium surrounding the anterior neuropore
927 (A.II). There is *Cep164* expression seen in the developing heart including the central
928 ventricle, bulbous cordis and outflow tract (A.III), as well as the developing limb buds
929 (A.IV). This *Cep164* expression pattern is maintained at E10.5 (B), *Cep164* expression is
930 seen in the optic cup and olfactory pit (B). At E12.5 *Cep164* expression is widespread but is

931 defined in the spinal cord, vertebrae, cerebral cortex, midbrain, hindbrain, pons and medulla
932 oblongata, otocyst and heart (C.I.II.III). *Cep164* expression is seen in the retina (C.IV) and at
933 the tips of the developing digits, where the apical ectodermal ridge is present
934 (C.V.VI.VII.VIII). WT littermates do not show endogenous beta galactosidase expression at
935 E9.5 (D.I), E10.5 (D.II), and E12.5 (F).
936
937 Anterior nucleopore (ANP), apical ectodermal ridge (AER), branchial arch (BA), bulbous
938 cordis (BC), cerebral cortex (CC), common atria (CA), common ventricle (CV), forebrain
939 (FB), forelimb bud (FL), heart (Ht), hindbrain (HB), hindlimb bud (HL), medulla oblongata
940 (MO), midbrain (MB), neural tube (NT), olfactory pit (OF), optic cup (OC), organ primordia
941 (Pri), otocyst (OT), outflow tract (OFT), pons (PO), somites (SM), spinal cord (SC), vertebral
942 column (VC).
943
944 **S4 Figure. Human CEP164 expression controls**
945 No primary antibody controls in the 8 PCW Kidney (A) and 18 PCW (B) kidney.
946 Renal vesicles, comma-shaped vesicles, S-Shaped body, uteric bud and cap mesenchyme
947 (A.I.II.III, B.I.II.III). Renal tubule and the renal corpuscle (A.IV.V.VII, B.IV.V.VI), Loop of
948 Henle and collecting ducts (B.VII). Lung, including the bronchioles and alveoli (C.I.II.III),
949 cardiomyocytes of the heart (C.I.IV,V), gastrointestinal tract (C.VI) and gonads (C.VII.VIII).
950 Dorsal root ganglia (C.VIX) and bone primordia (C.VX), liver (C.IX). Developing brain (D.I,
951 E.I) including the telencephalon (C.VI), metencephalon (C.V) and myencephalon (C.VIII).
952 Midline (D.II), and neuroepithelium surrounding the brain ventricles (C.VIII, D.III.IV).
953 Choroid plexus ependymal cells (C.II.III.IV) and choroid plexus pia matter (C.III.IV).
954 Molecular cell layer, Purkinje and ganglion cell layers of cerebellum (F.I.II). Ventricular

surface (F.III.IV), medulla oblongata (F.VI), and white matter (F.VII). Choroid plexus at 16 PCW (F.V). PAX9 positive control antibody (E.V, F.IX).

Alveoli primordia (Av Pri), bone primordia (BP), bronchiole (Br), cap mesenchyme (CM), cardiomyocyte (CM), cerebellum (Ce), choroid plexus (CP), collecting duct (CD), cortical plate (CorP), diencephalon (Di), dorsal root ganglia (DRG), ependymal cells (Ep), ganglion cell layer (GCL), gastrointestinal tract (GI), germline epithelium (GE), gonad (Go), intermediate Zone (IL), heart (Ht), hepatocytes (Hep), fourth ventricle (FV), kidney (Ki), lateral ventricle (LV), lamina propria (LM), liver (Li), loop of henle (LH), lung (Lu), marginal Layer (MaL), medulla oblongata (MO), mesencephalon (Mes), metencephalon (Met), midline (Mi), molecular Cell Layer (MCL), muscularis externa (ME), muscularis mucosae (MM), myencephalon (Mye), nasal epithelium (Na), pia (P), post conception weeks (PCW), purkinje cell layer (PCL), renal corpuscle (RC), renal tubules (RT), renal vesicle (RV), seminiferous cord (SC), s-shaped body (SSB), submucosae (SB), sub-ventricular layer (SVL), squamous epithelium mucosae (Mc-sq), telencephalon (Tel), uteric bud (UB), ventricular layer (VL), ventricular surface (VS), white matter (WM).

S5 Figure. Littermate WT controls for murine *Cep164* expression

(A) murine retina. (B-C) murine kidney (D) murine secondary tissues, (E-F) murine cerebellar tissues. Retina at P1.5 (A.I), P15.5 (A.II), and P29.5 (A.III). Renal vesicles (B.I.II.III), uteric bud (B.III), renal tubules (B.IV) and renal corpuscle (B.V.VI). Renal tissue at P30.5 has low endogenous beta galactosidase expression (C.I) in the renal tubules (C.III.IV), but not in the renal corpuscle (C.II). Developing brain (D.I), costal cartilage (D.II) and intercostal muscle (D.III). The P0.5 lung (E.I.II.III.IV), and alveoli (E.V), P30.5 murine lung trachea, bronchioles or alveoli (E.I.II.III.IV.V.VI). Murine heart, cardiomyocytes

(D.VI.VII, E.VI.VII), developing testes, spermatogonia, spermatocytes, spermatids and smooth muscle cells in the seminiferous tubules (D.VIII.IX.X, E.VIII.IX.X). Hepatocytes of the liver, hepatic portal vein (D.XI.XII.XIII, E.XI.XII.XIII). Murine brain cerebral hemisphere (F.I.V, G.I,H.I), the midbrain (F.VI,G.VII,,H.V), the striatum (G.V,) and thalamus (G.VI),H.VI).The choroid plexus shows some weak endogenous beta galactosidase expression (F.IV). Ganglion cell layer, molecular cell layer, Purkinje cell layer and white matter of the cerebellum (F.II.III.IV, G.II.III.IV, H.II.III).

Alveoli (Av), bronchiole (Br), cardiomyocyte (CM), cartilage (Ca), cerebellum (Ce), cerebral hemisphere (Ch), cerebrum (Cr), choroid plexus (CP), connective tissue (CT), costal cartilage (CC), epithelial (Ep), ganglion cell layer (GCL), heart (Ht), hepatocytes (Hep), inner nuclear layer (INL), inner plexiform layer (IPL), intercostal muscle (IC), liver (Li), lung (Lu), marginal layer (MaL), medulla oblongata (MO), midbrain (MB), molecular cell layer (MCL), outer neuroblastic layer (ONBL), outer nuclear layer (ONL), outer plexiform layer (OPL), photoreceptor segment layer (PS), pons (PO), postnatal day (P), purkinje cell layer (PCL), renal corpuscle (RC), renal tubule (RT), renal vesicle (RV), respiratory bronchiole (R), retinal pigment epithelium (RPE), seminiferous tubule (ST), smooth muscle (SM), spermatids (Sp), spermatocytes (SC), spermatogonia (Spg), striatum (St), terminal bronchi (TB), thalamus (Th), trachea (Tr), uteric bud (UB), white matter (WM).

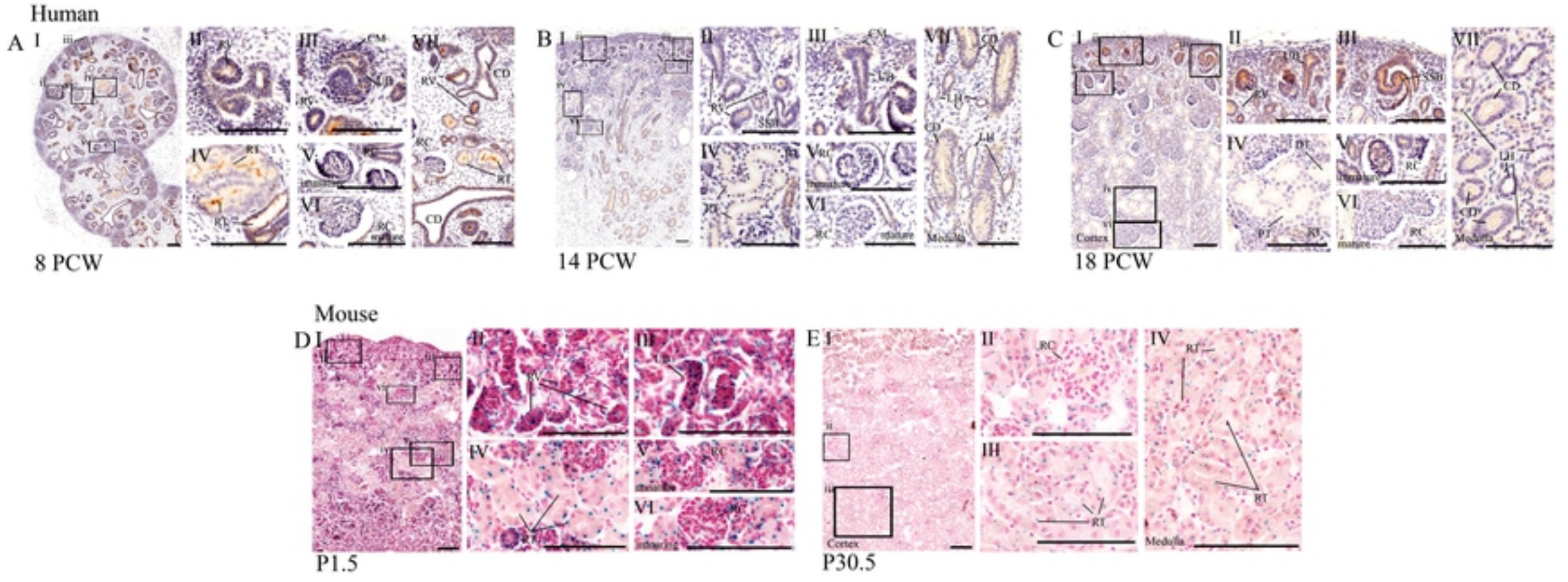

Figure

A Human

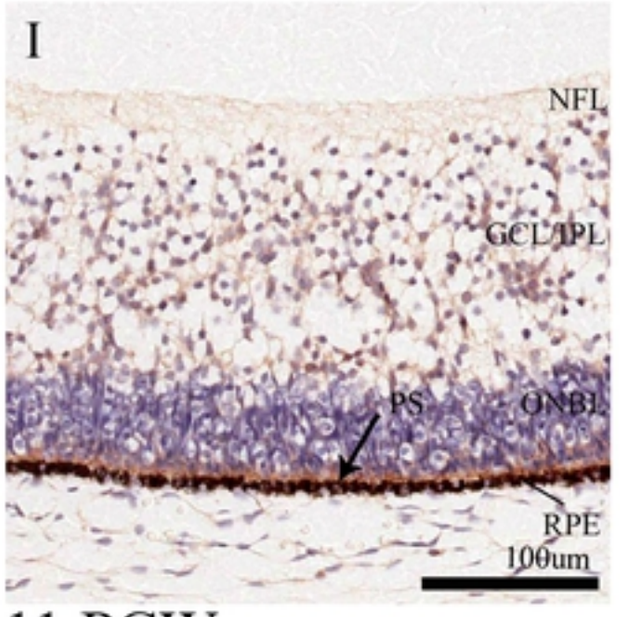

11 PCW

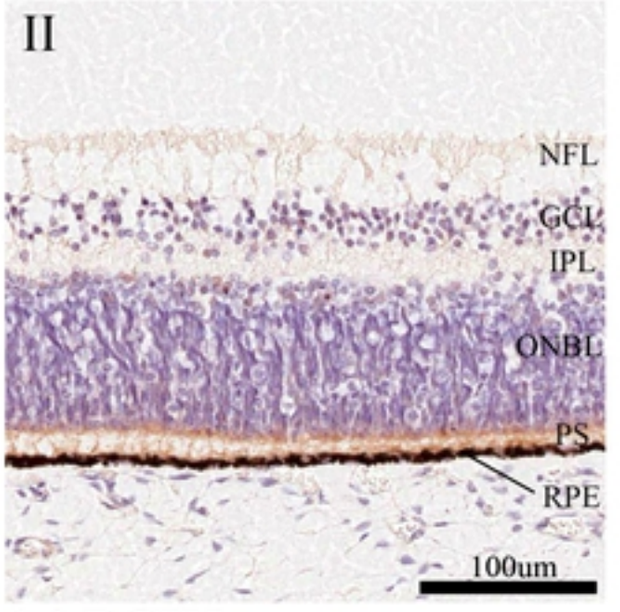

14 PCW

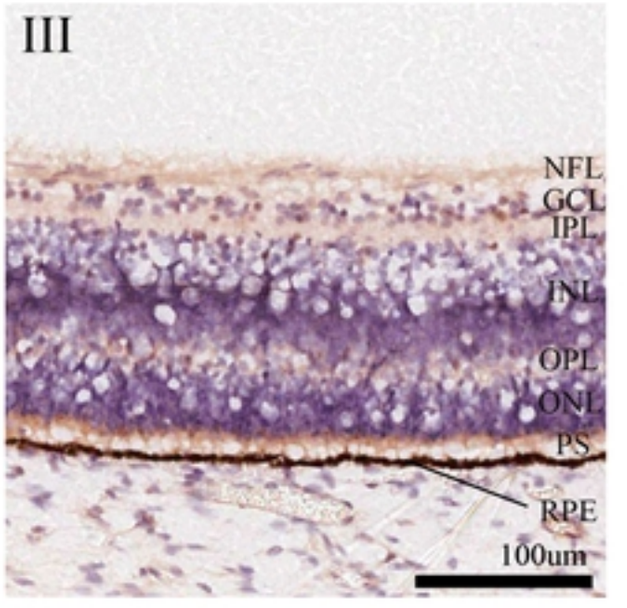

19 PCW

B Mouse

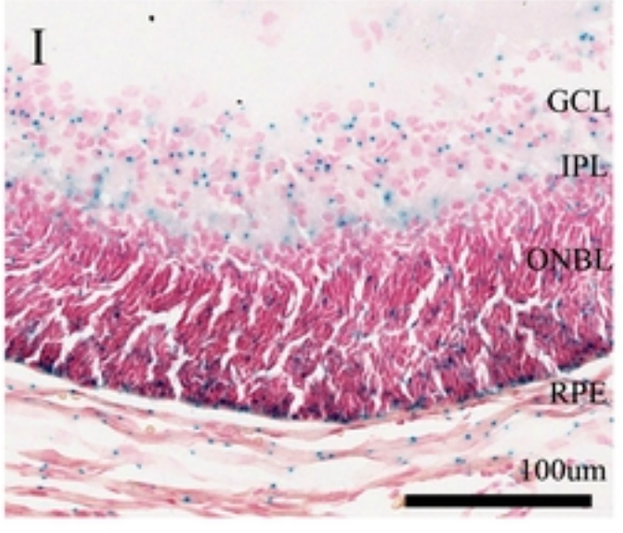

P1.5

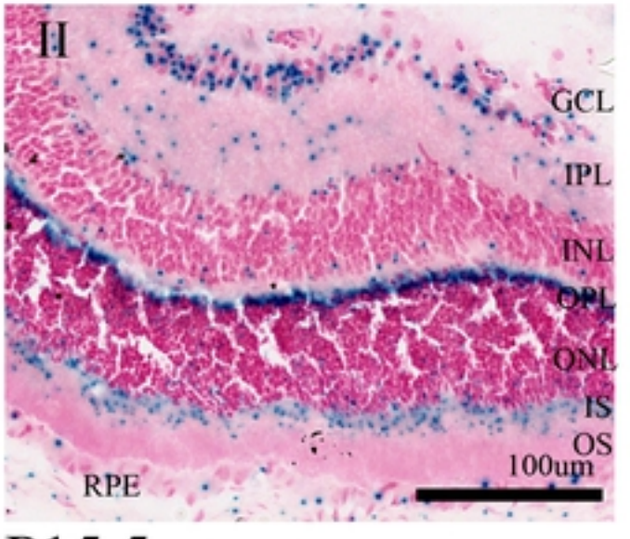

P15.5

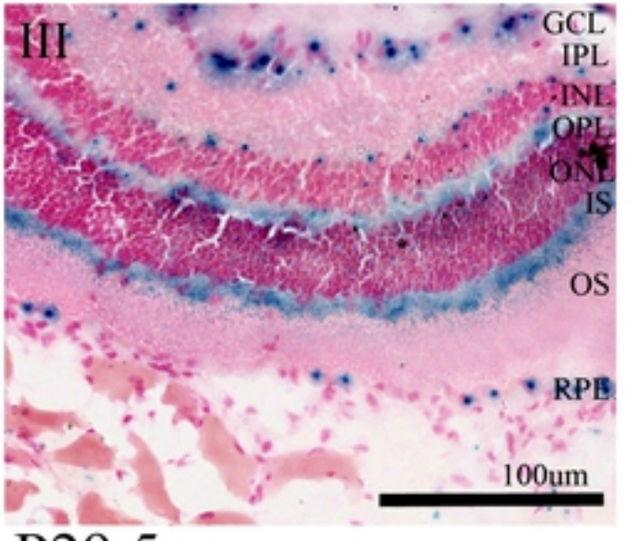

P29.5

Figure

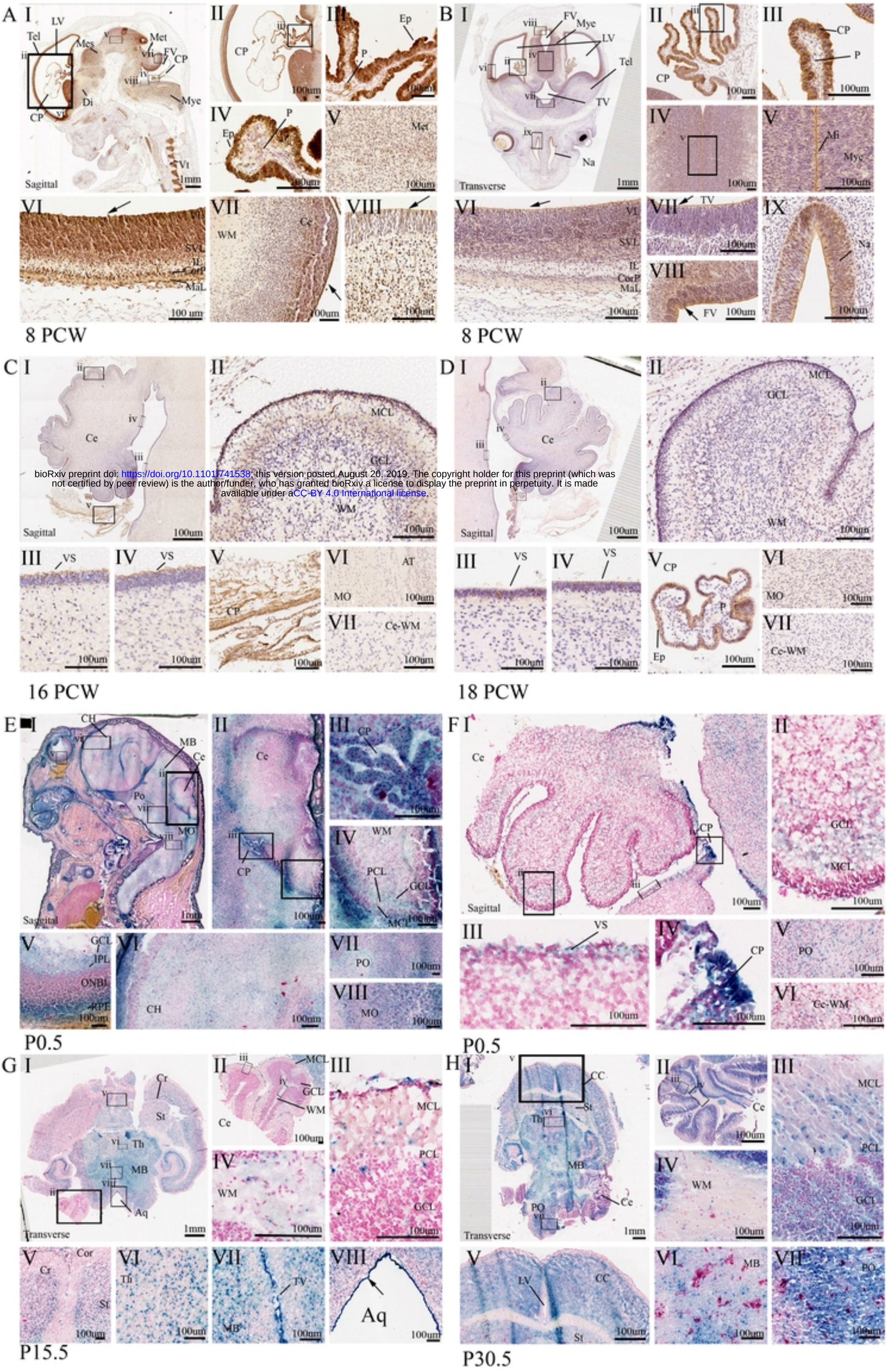

Figure

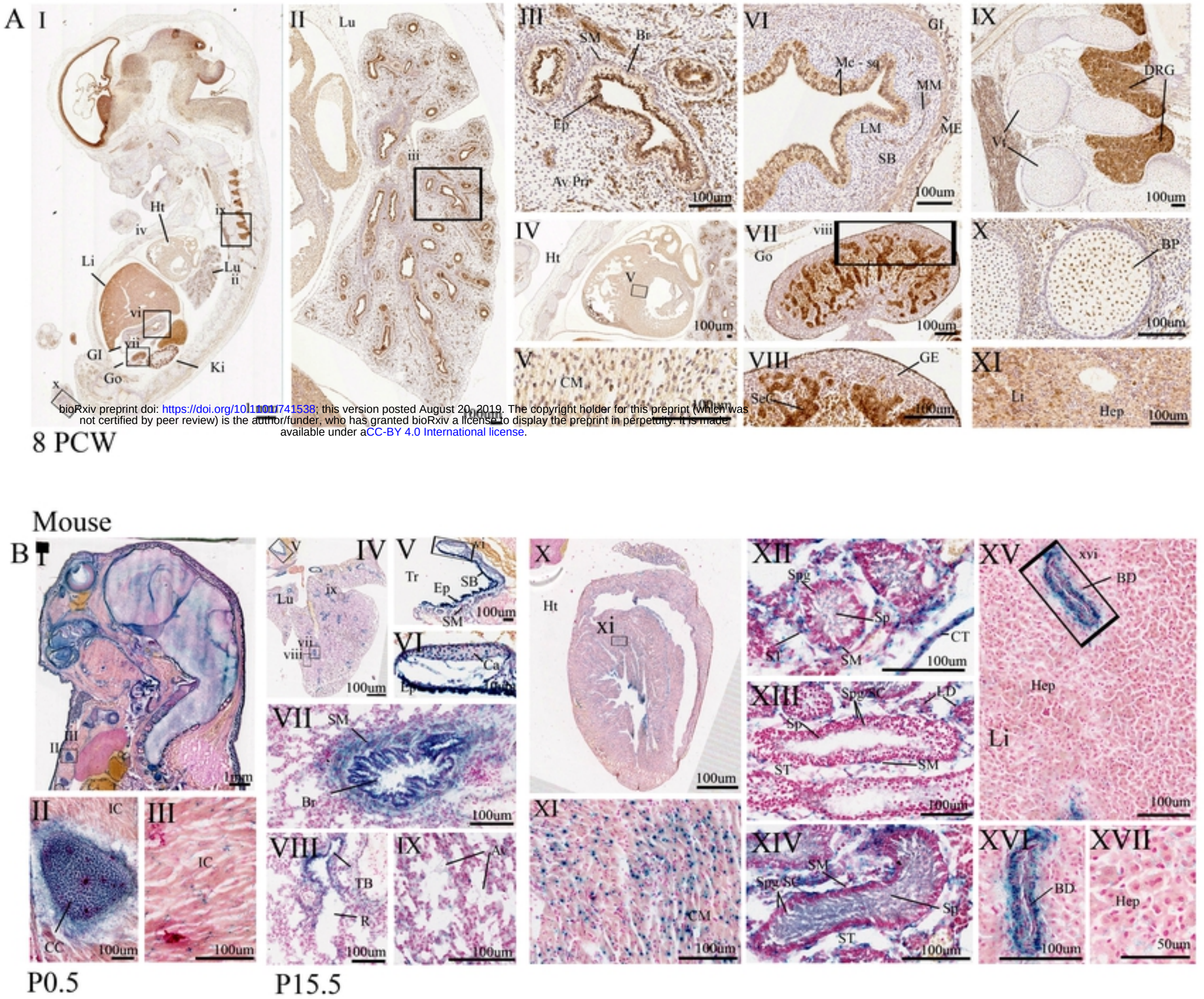

Figure